ACS Chemical Neuroscience

pubs.acs.org/chemneuro Research Article

Interplay of Cholesterol and Actin in Neurotransmitter GPCR Signaling: Insights from Chronic Cholesterol Depletion Using Statin

Parijat Sarkar and Amitabha Chattopadhyay*

Cite This: *ACS Chem. Neurosci.* 2023, 14, 3855−3868 Read Online

ACCESS | Metrics & More | Article Recommendations | Supporting Information

ABSTRACT: Serotonin$_{1A}$ receptors are important neurotransmitter receptors in the G protein-coupled receptor (GPCR) family and modulate a variety of neurological, behavioral, and cognitive functions. We recently showed that chronic cholesterol depletion by statins, potent inhibitors of HMG-CoA reductase (the rate-limiting enzyme in cholesterol biosynthesis), leads to polymerization of the actin cytoskeleton that alters lateral diffusion of serotonin$_{1A}$ receptors. However, cellular signaling by the serotonin$_{1A}$ receptor under chronic cholesterol depletion remains unexplored. In this work, we explored signaling by the serotonin$_{1A}$ receptor under statin-treated condition. We show that cAMP signaling by the receptor is reduced upon lovastatin treatment due to reduction in cholesterol as well as polymerization of the actin cytoskeleton. To the best of our knowledge, these results constitute the first report describing the effect of chronic cholesterol depletion on the signaling of a G protein-coupled neuronal receptor. An important message arising from these results is that it is prudent to include the contribution of actin polymerization while analyzing changes in membrane protein function due to chronic cholesterol depletion by statins. Notably, our results show that whereas actin polymerization acts as a negative regulator of cAMP signaling, cholesterol could act as a positive modulator. These results assume significance in view of reports highlighting symptoms of anxiety and depression in humans upon statin administration and the role of serotonin$_{1A}$ receptors in anxiety and depression. Overall, these results reveal a novel role of actin polymerization induced by chronic cholesterol depletion in modulating GPCR signaling, which could act as a potential therapeutic target.

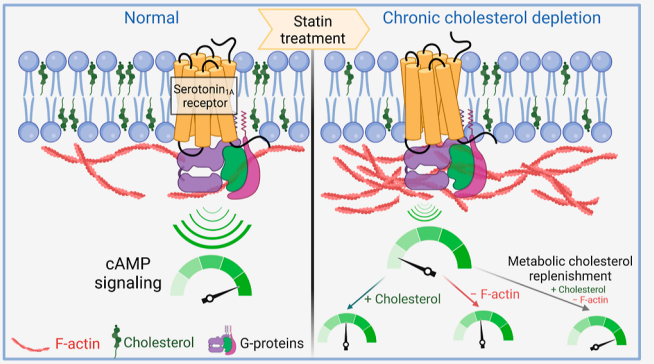

KEYWORDS: *actin polymerization, cAMP signaling, chronic cholesterol depletion, GPCR, serotonin$_{1A}$ receptor, statin*

INTRODUCTION

G protein-coupled receptors (GPCRs) are the largest and most diverse class of seven-transmembrane domain-membrane proteins ubiquitously present in eukaryotes.[1−3] They carry out a range of signal transduction processes across the plasma membrane as a result of binding to various extracellular ligands. The ligand binding events are followed by coordinated structural changes in their transmembrane and extramembranous regions, which lead to relay of signals to the cellular interior.[4−6] Since signaling by GPCRs is involved in a large number of physiological processes ranging from development to cancer; they serve as major drug targets in all clinical areas.[7−10] Although traditionally, GPCR signaling was viewed as a chain of events initiated from the plasma membrane, recent evidence suggests that internalized pool of GPCRs could also mediate signaling that is different from that on the plasma membrane.[11−14] This further opens up new opportunities to develop novel therapeutic approaches to target GPCRs.[15,16] The serotonin$_{1A}$ receptor is an important neurotransmitter receptor in the GPCR superfamily, which modulates a multitude of neurological, behavioral, and cognitive functions[17−22] and is a prominent drug target for treating neuropsychiatric disorders and even cancer.[23,24]

Since GPCR signaling involves functional interaction of molecules separated spatiotemporally; lateral dynamics of these components in the membrane acts as a determinant of cellular signaling by them. This aspect of receptor-mediated signaling was first conceptualized by the "mobile receptor" hypothesis.[25−27] Keeping in mind the heterogeneity of cellular membranes[28] and the dynamic nature of organization of membrane-bound molecules,[29] it is evident that functional association between GPCRs and their effectors would be largely governed by the probabilities of their interactions. Consequently, receptor dynamics (lateral diffusion) in membranes determines overall efficacy of the signal trans-

Received: July 14, 2023
Accepted: September 25, 2023
Published: October 7, 2023

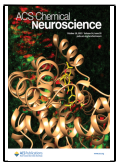

https://doi.org/10.1021/acschemneuro.3c00472
ACS Chem. Neurosci. 2023, 14, 3855−3868

duction process.[30−32] In this overall context, measurement of live cell membrane dynamics, with the objective of correlating it with receptor signaling, assumes relevance. Interestingly, the actin cytoskeleton has emerged as a modulator of mobility (lateral diffusion) of membrane proteins in the plasma membrane[33−36] and dynamic reorganization of the actin cytoskeleton has been shown to modulate GPCR signaling.[32,35]

We recently showed that chronic cholesterol depletion by statins leads to polymerization of the cellular actin cytoskeleton,[37] which results in altered lateral diffusion of the serotonin$_{1A}$ receptor.[38] In this work, we probed the interdependence between actin polymerization and signaling by the serotonin$_{1A}$ receptor in response to chronic cholesterol depletion. For this, we explored the effect of lovastatin on the function of the human serotonin$_{1A}$ receptor, which was stably expressed in Chinese hamster ovary (CHO) cells. Our results show a dose-dependent reduction in specific agonist binding to the serotonin$_{1A}$ receptor upon chronic cholesterol depletion, which was reversed upon cholesterol replenishment. Notably, downstream cAMP signaling by the serotonin$_{1A}$ receptor was impaired upon chronic cholesterol depletion, although the total receptor level did not exhibit any significant reduction. We further show that the inhibitory effect of statins on GPCR signaling is due to a combination of reduced membrane cholesterol and constrained dynamics (due to actin polymerization) of the receptor in cholesterol-depleted condition. Specifically, we propose that reorganization of the actin cytoskeleton may contribute to this effect, a mechanism not previously reported in the literature. Our results show the modulation of signaling by GPCR-cytoskeleton interactions, highlighting the importance of considering the actin cytoskeleton as a crucial player in analyzing the role of the membrane environment in the function of membrane proteins. These novel results have significant implications in understanding the influence of cholesterol lowering agents such as statins on cellular signaling of GPCRs in healthy and diseased states.

RESULTS

Chronic Cholesterol Depletion Using Lovastatin. To explore the effect of chronic cholesterol depletion on the function of the human serotonin$_{1A}$ receptor, we depleted cholesterol from CHO-K1 cells using lovastatin. Statins have emerged as best-selling oral cholesterol-lowering drugs and offer a useful handle to deplete cell membrane cholesterol in vitro in a physiological fashion.[39−41] Statins competitively inhibit the rate-limiting enzyme HMG-CoA reductase in cellular cholesterol biosynthesis pathway.[42,43] Unlike acute depletion methods [such as extraction of cholesterol using carriers such as methyl-β-cyclodextrin (MβCD)], cholesterol depletion by statins takes place at a longer time scale that mimics physiological conditions.[44−46] Notably, we previously showed that the consequences of membrane cholesterol depletion could depend on the actual method (acute vs chronic) of cholesterol removal.[37,47−50] The effect of chronic cholesterol depletion on cellular signaling by the serotonin$_{1A}$ receptor remains unexplored from this perspective. Figure 1A shows the cholesterol content in cells treated with increasing concentrations of lovastatin for 48 h. The figure shows a concentration-dependent reduction in cellular cholesterol content, with maximum reduction (~36%) upon treatment with 10 μM lovastatin. Changes in total phospholipid content under these conditions were negligible (Figure S1A),

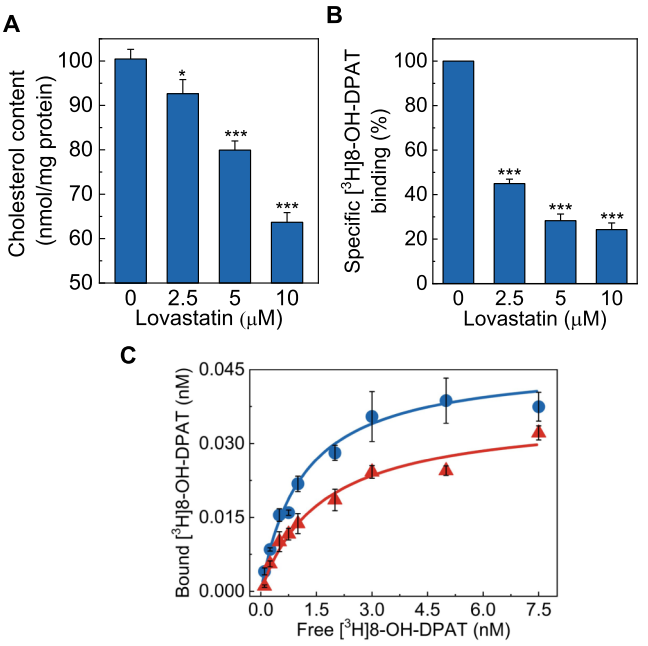

Figure 1. Ligand binding activity of the human serotonin$_{1A}$ receptor is reduced upon chronic cholesterol depletion. (A) Cholesterol content of CHO-K1 cells treated with increasing concentrations of lovastatin. Values are expressed as absolute cholesterol content in membranes and are normalized to total protein content. Data represent means ± SE of three independent experiments (* and *** correspond to significant difference ($p < 0.05$ and $p < 0.001$, respectively) in cholesterol content in lovastatin-treated cells relative to untreated cells). (B) Binding of the specific agonist [^{3}H]8-OH-DPAT to serotonin$_{1A}$ receptors in live CHO-K1 cells treated with increasing concentrations of lovastatin. Nonspecific binding was obtained by performing the assay in the presence of unlabeled serotonin. Ligand binding values were normalized relative to control (untreated cells). Data represent means ± SE from at least four independent experiments (*** corresponds to significant ($p < 0.001$) difference in specific [^{3}H]8-OH-DPAT binding in cells treated with lovastatin relative to untreated cells). (C) Saturation binding analysis of specific [^{3}H]8-OH-DPAT binding to the serotonin$_{1A}$ receptor in live cells. The saturation binding data could be fitted best to a one-site ligand binding equation. Binding plots are shown for control (blue ●) and 2.5 μM lovastatin-treated (red ▲) cells. The curves are nonlinear regression fits to the experimental data using eq 2. Data represent means ± SE of three independent experiments. See Table 1 and Methods for more details.

indicating that lovastatin treatment is specific to reduction in cellular cholesterol. In addition, membrane lipid contents of control and lovastatin-treated cells were analyzed by thin layer chromatography (TLC) and showed no changes in phospholipid composition upon chronic cholesterol depletion (Figure S1B). The ranges of lovastatin concentration and treatment duration were chosen carefully to avoid any compromise in cell viability.[37]

Ligand Binding of the Serotonin$_{1A}$ Receptor Is Reduced upon Chronic Cholesterol Depletion. We monitored ligand binding of the serotonin$_{1A}$ receptor upon lovastatin treatment in CHO-K1 cells expressing the human serotonin$_{1A}$ receptor tagged to enhanced yellow fluorescent protein to the C-terminus (abbreviated as CHO-K1-5HT$_{1A}$R-EYFP). Previous work from our laboratory has shown that enhanced yellow fluorescent protein (EYFP) fusion to the serotonin$_{1A}$ receptor at the carboxy terminal does not affect

https://doi.org/10.1021/acschemneuro.3c00472
ACS Chem. Neurosci. 2023, 14, 3855−3868

ligand binding, G-protein coupling, and signaling of the receptor, and the EYFP-tagged receptor mimics the pharmacological and signaling features of the receptor.[51] We measured binding of the specific agonist [^{3}H]8-OH-DPAT to serotonin$_{1A}$ receptors in live cells. For this, we carried out radioligand binding in intact cells (not isolated cell membranes) since the process of isolation of cell membranes could affect the organization of the underlying cytoskeleton. Figure 1B shows that cholesterol depletion with an increasing lovastatin concentration led to dose-dependent reduction in specific agonist [^{3}H]8-OH-DPAT binding to serotonin$_{1A}$ receptors. For example, specific agonist binding was reduced by ∼76% relative to untreated (control) cells when cells were treated with 10 μM lovastatin.

The observed reduction in specific agonist binding to serotonin$_{1A}$ receptors upon statin treatment (Figure 1B) could be due to either a reduction in affinity or loss in ligand binding sites or a combination of both effects. To gain further insight into the mechanism of reduction in agonist binding in cholesterol-depleted condition, we carried out saturation binding assays. Representative binding plots from saturation binding analysis for binding of the specific agonist ([^{3}H]8-OH-DPAT) in control cells and cells treated with 2.5 μM lovastatin are shown in Figure 1C. Data from saturation binding assays were analyzed using eq 2, and values of binding parameters [i.e., equilibrium dissociation constant (K_d) and maximum binding sites (B_{max})] are shown in Table 1. Our analysis showed that K_d was 1.16 nM in untreated cells, whereas a considerably higher K_d of 1.80 nM was obtained for cells treated with 2.5 μM lovastatin. This shows a reduction in agonist binding affinity to serotonin$_{1A}$ receptors under cholesterol-depleted condition, as indicated by the significant increase in K_d value (see Table 1). This was accompanied by a reduction (∼33%) in the number of maximum binding sites (B_{max}) when cells were treated with 2.5 μM lovastatin (Table 1). Analysis of binding curves yielded a B_{max} value of 49 fmol/10^6 cells in untreated cells, whereas treatment with lovastatin resulted in a significantly lower B_{max} value of 33 fmol/10^6 cells (Table 1). Taken together, the reduction in specific agonist binding (Figure 1B) could be attributed to a combination of reduction in binding affinity and binding sites in serotonin$_{1A}$ receptors upon chronic cholesterol depletion.

Table 1. Effect of Chronic Cholesterol Depletion on Specific [^{3}H]8-OH-DPAT Binding to Serotonin$_{1A}$ Receptors[a]

condition	K_d (nM)	B_{max} (fmol/10^6 cells)
control	1.16 ± 0.06	49 ± 3
treated with 2.5 μM lovastatin	1.80 ± 0.13[b]	33 ± 1[b]

[a]The binding parameters shown represent means ± SE from three independent experiments, whereas saturation binding data shown in Figure 1C are from a representative experiment. See Methods for more details. [b]A significant decrease in K_d and B_{max} ($p < 0.05$) was observed relative to control cells.

Expression Level of the Serotonin$_{1A}$ Receptor Remains Unchanged under Statin-Treated Condition. The impaired ligand binding function of the serotonin$_{1A}$ receptor observed upon treatment with lovastatin could be due to the reduced expression levels of receptors upon cholesterol depletion. To check this, we performed flow cytometric analysis of CHO-K1-5HT$_{1A}$R-EYFP cells under control and cholesterol-depleted conditions (see Figure 2A). The figure shows representative flow cytometric histograms with a staggered overlay of fluorescence intensity, indicating invariance of the total serotonin$_{1A}$ receptor population under control and cholesterol-depleted conditions. It should be noted that since the fluorescence of EYFP originates from both plasma membrane and internal membrane-associated population of serotonin$_{1A}$ receptors, our flow cytometry-based assay reports the total expression level of the serotonin$_{1A}$ receptor. Importantly, as recently showed by us,[38] cellular distribution of serotonin$_{1A}$ receptors was not affected due to statin treatment. These results show that chronic cholesterol depletion does not induce any significant change in the expression levels of serotonin$_{1A}$ receptors.

Differential Ligand Binding Is Not Due to Endocytosis of the Serotonin$_{1A}$ Receptor. As mentioned above, we carried out radioligand binding experiments in live cells to examine any synergistic role of the actin cytoskeleton in modulating the functional outputs of the receptor. This raises the possibility that the radiolabeled agonist could drive receptor endocytosis and contribute to a difference in ligand binding activity in lovastatin-treated cells relative to control cells. This prompted us to set up additional experiments to address this question. Interestingly, previous work from our laboratory has shown that chronic cholesterol depletion does not affect the extent of internalization of the serotonin$_{1A}$ receptor in HEK-293 cells heterologously expressing the serotonin$_{1A}$ receptor.[48] To rule out any effect of receptor endocytosis during the time of incubation with radiolabeled agonist (or serotonin during estimation of nonspecific binding), we pretreated cells with an inhibitor of ATP synthesis prior to radioligand binding experiments. We previously showed that treatment with 10 mM sodium azide (inhibitor of ATP synthesis) inhibits endocytosis of the serotonin$_{1A}$ receptor.[52] Figure 2B shows that the effect of endocytosis on the specific ligand binding of the serotonin$_{1A}$ receptor was negligible, as evident from similar extents of reduction in ligand binding across all conditions. Taken together, these results indicate that the reduction in radioligand binding to the serotonin$_{1A}$ receptor was not due to endocytosis of the receptor.

Reduction in Ligand Binding upon Chronic Cholesterol Depletion Is Reversible in Nature. Next, we explored the reversibility of the changes induced by chronic cholesterol depletion upon ligand binding of the serotonin$_{1A}$ receptor by replenishment of cholesterol in lovastatin-treated cells. For this, we metabolically replenished cholesterol in lovastatin-treated cells by washing off the lovastatin-containing medium and further incubating cells with complete culture medium without lovastatin. Figure 2C shows that incubation of cholesterol-depleted cells in medium containing serum replenishes cholesterol to normal levels, as shown by the cholesterol content of replenished cells. We then monitored the corresponding recovery in ligand binding under these conditions (Figure 2D). The figure shows that metabolic replenishment of cholesterol resulted in complete recovery of ligand binding to the serotonin$_{1A}$ receptor. These results show that the loss of ligand binding upon chronic cholesterol depletion is reversible in nature.

Signaling by the Serotonin$_{1A}$ Receptor Is Compromised upon Chronic Cholesterol Depletion. As a downstream effect of agonist binding, the serotonin$_{1A}$ receptor has been shown to activate the Gi/Go class of G-proteins in CHO-K1 cells,[53−55] which results in the inhibition of adenylyl

https://doi.org/10.1021/acschemneuro.3c00472
ACS Chem. Neurosci. 2023, 14, 3855−3868

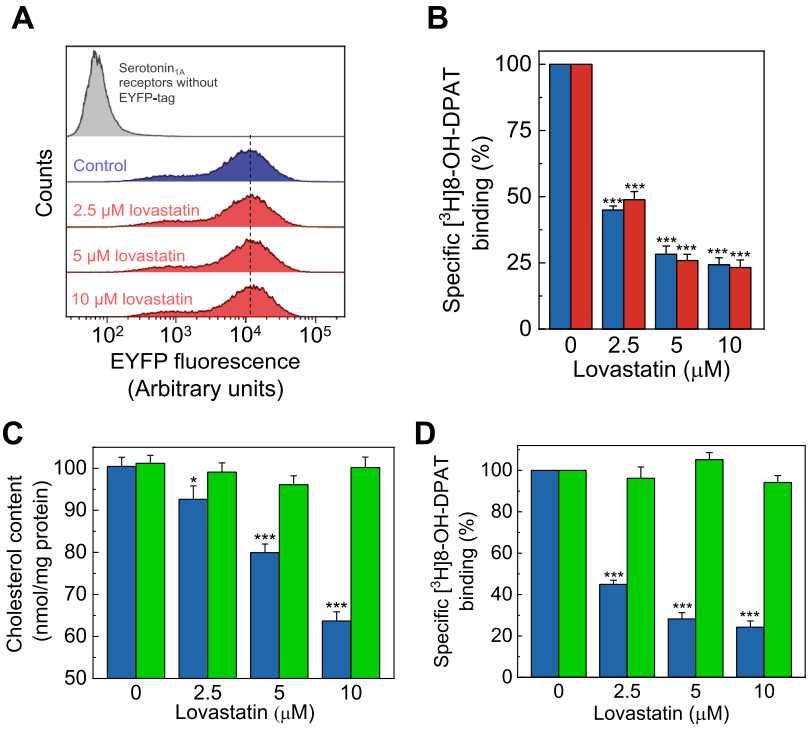

Figure 2. (A) Staggered overlay of representative flow cytometric histograms indicating the total population of serotonin$_{1A}$ receptors corresponding to control (blue) and lovastatin-treated cells (red). The serotonin$_{1A}$ receptor tagged with EYFP at the C-terminal and heterologously expressed in CHO-K1 cells was utilized for this analysis. Fluorescence from cells expressing the serotonin$_{1A}$ receptor without the EYFP tag was used to gate EFYP-positive cells and is represented as a gray histogram toward lower value on the fluorescence axis. (B) Binding of the specific agonist [^{3}H]8-OH-DPAT to serotonin$_{1A}$ receptors in lovastatin-treated CHO-K1 cells under control (blue) and azide-treated (red) conditions. Endocytosis was inhibited by pretreating cells with 10 mM sodium azide (inhibitor of ATP synthesis) for 30 min prior to radioligand binding experiments. Ligand binding values are normalized relative to respective control cells (without lovastatin). Data represent means ± SE from three independent experiments (*** corresponds to significant ($p < 0.001$) difference in specific [^{3}H]8-OH-DPAT binding in lovastatin-treated cells relative to untreated cells under control and azide-treated conditions). (C) Cholesterol content in CHO-K1 cells under cholesterol-depleted (blue) and cholesterol-replenished (green) conditions. Cholesterol was metabolically replenished in lovastatin-treated cells by incubating cells with complete medium in the absence of lovastatin. Values are expressed as absolute cholesterol content and are normalized to the total protein content. Data of membrane cholesterol content for lovastatin-treated cells are taken from Figure 1A. Data represent means ± SE of three independent experiments (* and *** correspond to significant difference ($p < 0.05$ and $p < 0.001$, respectively) in membrane cholesterol content in lovastatin-treated cells relative to untreated cells). (D) Binding of the specific agonist [^{3}H]8-OH-DPAT to serotonin$_{1A}$ receptors upon cholesterol replenishment (green) condition. Ligand binding values are normalized with respect to respective control cells (in the absence of lovastatin). Data of specific agonist binding in lovastatin-treated cells (blue) are taken from Figure 1B. Data represent means ± SE from three independent experiments (*** corresponds to significant ($p < 0.001$) difference in specific [^{3}H]8-OH-DPAT binding in lovastatin-treated cells relative to untreated cells). See Methods for more details.

cyclase activity that leads to reduction in cellular cAMP levels. To explore the effect of chronic cholesterol depletion on signaling by the serotonin$_{1A}$ receptor, we monitored the effect of serotonin-stimulation on cAMP levels in CHO-K1 cells expressing the serotonin$_{1A}$ receptor utilizing a FRET-based assay.[56−58] Since basal levels of cAMP are insufficient to measure this signaling, the cellular cAMP level needs to be elevated (with agents such as forskolin that directly activate adenylyl cyclase) for estimation of Gαi-mediated signaling. As a result, this assay relies on estimating the serotonin-induced reduction in forskolin-stimulated cAMP levels. In addition, we used the phosphodiesterase inhibitor IBMX during all treatments to prevent the breakdown of cAMP by cellular phosphodiesterases. As shown in Figure 3A, forskolin-stimulation resulted in ∼127% increase in cellular cAMP level relative to nonstimulated (only IBMX) cells. Subsequent reduction in cAMP levels in forskolin-treated cells upon stimulation with serotonin was used as a measure of the efficiency of signaling by the receptor. In the absence of lovastatin, treatment with 10 μM serotonin suppressed forskolin-stimulated enhancement of cAMP levels, suggesting the expression of functional serotonin$_{1A}$ receptor in CHO-K1 cells (Figure 3A).

To explore the effect of chronic cholesterol depletion on serotonin$_{1A}$ receptor signaling, we measured serotonin-induced reduction in cAMP levels in cells treated with increasing concentrations (2.5−10 μM) of lovastatin (Figure 3B−D). Figure 3 shows that treatment with increasing concentrations of lovastatin suppressed the ability of serotonin to reduce cAMP levels in a dose-dependent manner. The reduction in cAMP levels upon serotonin treatment relative to forskolin-stimulated levels was quantified from Figure 3B−D and is shown in Figure 3E. The figure shows that control (in the absence of lovastatin) cells exhibited ∼112% reduction in cAMP levels upon treatment with serotonin. Interestingly, serotonin-induced reduction in cAMP levels exhibited a progressive reduction upon treatment with increasing concentrations of lovastatin. This implies that chronic cholesterol depletion inhibits signaling by the human serotonin$_{1A}$ receptor. Notably, the stimulatory effect of forskolin on cAMP synthesis

https://doi.org/10.1021/acschemneuro.3c00472
ACS Chem. Neurosci. 2023, 14, 3855−3868

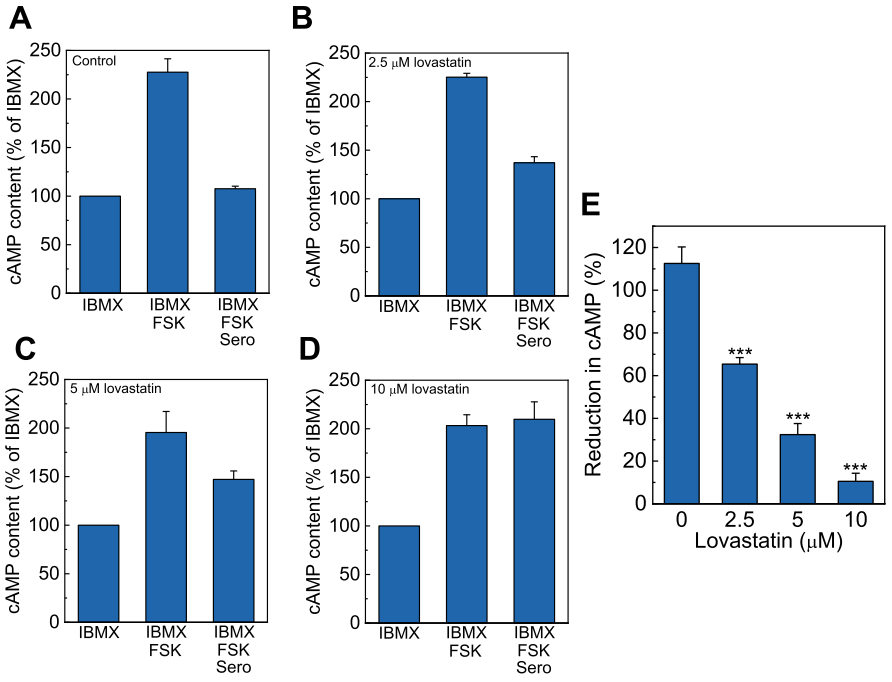

Figure 3. Estimation of cellular cAMP levels in CHO-K1 cells heterologously expressing human serotonin$_{1A}$ receptors. The ability of the serotonin$_{1A}$ receptor to inhibit forskolin-stimulated increase in cAMP levels upon treatment with 10 μM serotonin was assessed under (A) control and (B−D) lovastatin-treated conditions. After treatment with lovastatin, cells were treated with 50 μM IBMX (basal) or 50 μM IBMX/10 μM forskolin (forskolin-stimulated) or 50 μM IBMX/10 μM forskolin/10 μM serotonin (agonist treatment). The phosphodiesterase inhibitor IBMX was present during all treatments to prevent breakdown of cAMP by cellular phosphodiesterases. The ability of the serotonin$_{1A}$ receptor to inhibit the forskolin-stimulated increase in cAMP levels was assessed using the FRET-based HTRF cAMP-Gi assay. Data are normalized to cAMP levels in the presence of IBMX for each condition. Data represent means ± SE of at least three independent experiments. (E) Chronic cholesterol depletion leads to reduction of cellular signaling by the human serotonin$_{1A}$ receptor. The figure shows the extent of reduction in forskolin-stimulated levels of cAMP in CHO-K1 cells expressing the serotonin$_{1A}$ receptor upon activation by 10 μM serotonin with increasing concentrations of lovastatin. Data are normalized to cAMP levels in the presence of 50 μM IBMX/10 μM forskolin (forskolin-stimulated) for each condition. Data represent means ± SE of at least three independent experiments [*** corresponds to significant ($p < 0.001$) difference in cAMP content under serotonin-treated condition for cells treated with lovastatin relative to control (in the absence of lovastatin) cells]. See Methods for more details.

appears to be comparable in normal and lovastatin-treated cells (Figure 3A−D). This ensures that cholesterol-depleted cells generate similar levels of cAMP relative to control (in the absence of lovastatin) cells in response to 10 μM forskolin. To the best of our knowledge, these results represent the first observation that chronic cholesterol depletion using statin leads to loss of cellular signaling mediated by the serotonin$_{1A}$ receptor.

Regulation of Signaling by the Human Serotonin$_{1A}$ Receptor. We further explored the mechanism underlying the reduction of cellular signaling by the serotonin$_{1A}$ receptor under cholesterol-depleted condition. As discussed above, the overall efficiency of GPCR signaling in membranes relies on the lateral dynamics (diffusion) of the activated receptor that represents an important determinant in its encounter with effectors (such as G-proteins).[27] In this context, the observed decrease in signaling by the serotonin$_{1A}$ receptor could arise due to reduction in lateral dynamics of the receptor upon chronic cholesterol depletion due to polymerization of the actin cytoskeleton (Figure 4).[37,38] On the other hand, another possibility could be direct interaction of cholesterol with the serotonin$_{1A}$ receptor necessary for its function.[58,59] To test these possibilities, we chose a two-pronged approach (Figure 5A). First, we explored the effect of increased F-actin (as a consequence of chronic cholesterol depletion) on signaling by the serotonin$_{1A}$ receptor in cholesterol-depleted cells. For this, we induced depolymerization of F-actin using cytochalasin D (CD, a potent inhibitor of actin polymerization)[60,61] subsequent to lovastatin-treatment (Figure 5A). We utilized a sub-μM concentration of CD (0.5 μM) that could effectively restore F-actin levels in lovastatin-treated cells similar to control levels. Figure 4A shows confocal micrographs showing the organization of F-actin in control and cells treated with increasing concentrations of lovastatin. The figure shows representative maximum intensity projections from confocal micrographs showing cellular F-actin and the corresponding iso-surface images (defined as contours made upon joining voxels of equal fluorescence intensity) in control cells and upon chronic cholesterol depletion using increasing concentrations of lovastatin. To estimate F-actin content under these conditions, we normalized the volume enclosed by the iso-surface in each case and normalized to the projected area of cells (Figure 5B). As shown in Figure 5B (blue bars), treatment with lovastatin led to polymerization of the actin cytoskeleton in a dose-dependent fashion. Figure 4B shows representative maximum intensity projections of F-actin in cells treated with 0.5 μM CD following treatment with increasing concentrations of lovastatin (2.5−10 μM). Values of F-actin content under these conditions are shown in Figure 5B (yellow bars). As shown in the figure, treatment with 0.5 μM CD in cholesterol-depleted cells led to significant reduction of F-actin content relative (yellow bars) to a corresponding value with lovastatin treatment alone (blue bars). The resultant F-actin content in these cells (cholesterol-depleted followed by

https://doi.org/10.1021/acschemneuro.3c00472
ACS Chem. Neurosci. 2023, 14, 3855−3868

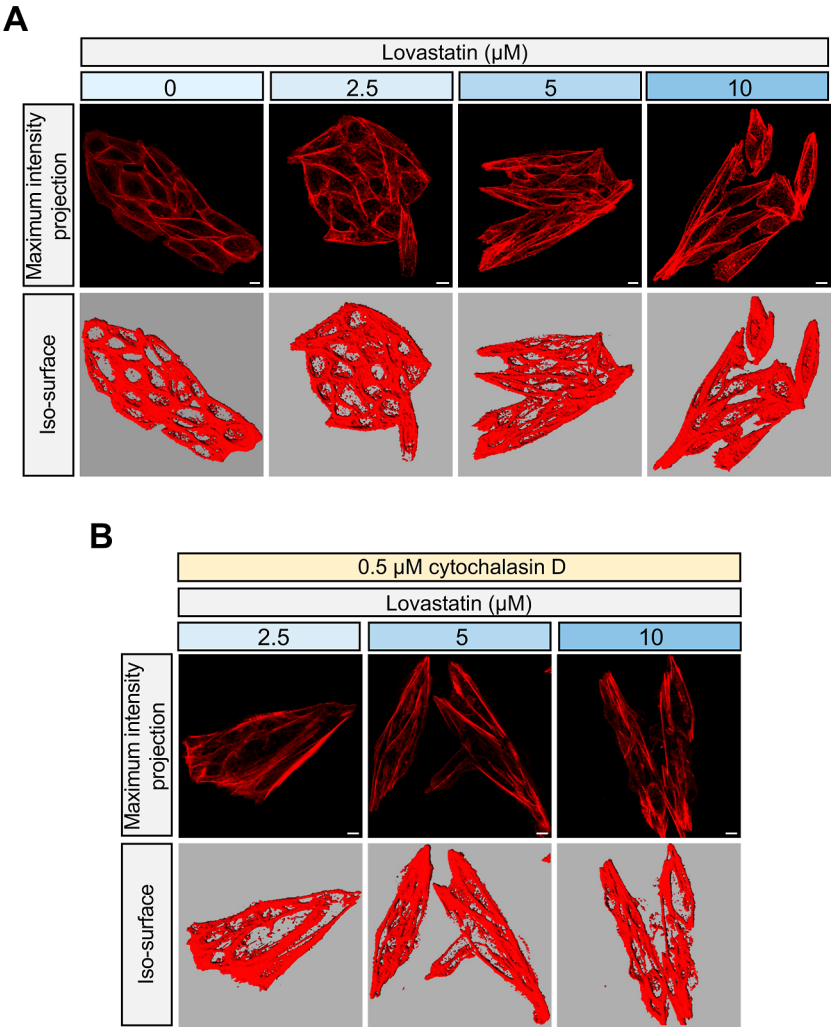

Figure 4. Chronic cholesterol depletion leads to polymerization of actin cytoskeleton. (A) Representative confocal micrographs showing organization of F-actin in control cells and cells treated with increasing concentrations of lovastatin. F-actin was stained with Alexa Fluor 546 conjugated phalloidin. The maximum intensity projections (MIPs) of 11 *z*-sections from the base of the coverslip (~3.5 μm from the base into the cell) are shown in the top panels. Increase in F-actin filaments can be observed upon treatment with increasing concentrations of lovastatin. Panels at the bottom represent the iso-surfaces (defined as voxel contours of equal fluorescence intensity) generated from the *z*-sections using the iso-surface tool in Imaris (Bitplane AG, Zurich, Switzerland) corresponding to MIPs shown on the top panels. (B) Organization of F-actin in CHO-K1 cells treated with 0.5 μM CD for 10 min in serum-free culture medium subsequent to chronic cholesterol depletion using lovastatin. F-actin was stained and quantified as described in (A). Scale bars represent 10 μm. See Methods for more details.

cytoskeleton-destabilized) was similar to the F-actin content in control cells (gray bar in Figure 5B). Importantly, acute treatment with CD subsequent to chronic cholesterol depletion had no significant effect on the cellular membrane cholesterol content (Figure 5C). Taken together, destabilization of the actin cytoskeleton could therefore provide a useful handle to explore cytoskeleton-dependent signaling by the serotonin$_{1A}$ receptor in cholesterol-depleted cells.

In an alternate approach, to explore the contribution of membrane cholesterol in the signaling by the serotonin$_{1A}$ receptor, we replenished membrane cholesterol in cells that were subjected to chronic cholesterol depletion (Figure 5A). We incubated lovastatin-treated cells with a preformed cholesterol−MβCD complex, which serves as a water-soluble carrier for membrane cholesterol and leads to cholesterol incorporation in cholesterol-deficient membranes. As shown in Figure 5D, treatment with the cholesterol−MβCD complex restored cholesterol levels in lovastatin-treated cells to control levels (compare the gray and red bars in Figure 5D). More importantly, such an acute replenishment of cholesterol had no additional effect on the F-actin content in lovastatin-treated cells (Figure 5E). In other words, this approach allows us to exclusively monitor the role of membrane cholesterol in the signaling of the serotonin$_{1A}$ receptor in cholesterol-depleted cells without altering the overall F-actin content.

We then monitored the effect of membrane cholesterol replenishment and actin destabilization on signaling by the human serotonin$_{1A}$ receptor using the two approaches described above. Figure 6A shows that acute replenishment of membrane cholesterol (red bars) led to partial recovery of serotonin$_{1A}$ receptor signaling relative to untreated cells (gray bar). For example, acute replenishment of membrane cholesterol restored reduction in cAMP content in 2.5, 5, and 10 μM lovastatin-treated cells to 96, 78, and 44%, respectively. It should be noted that although the membrane cholesterol content in lovastatin-treated cells could be restored to a level similar to that in untreated cells (see Figure 5D), we could observe only a partial recovery of cellular signaling after

https://doi.org/10.1021/acschemneuro.3c00472
ACS Chem. Neurosci. 2023, 14, 3855−3868

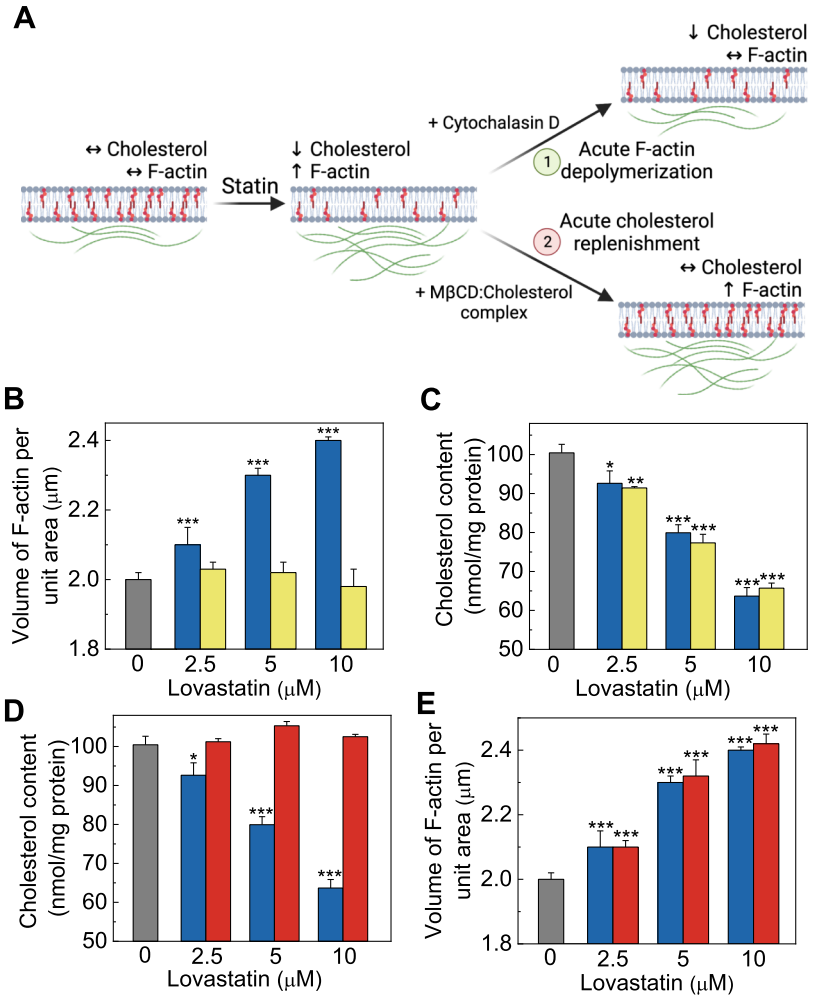

Figure 5. (A) Chronic cholesterol depletion by statin leads to reduction in membrane cholesterol (shown in red) and polymerization of the actin cytoskeleton (shown as green meshwork underlying the membrane). Using a two-pronged approach, we dissected the role of membrane cholesterol and cellular F-actin in signaling of the serotonin$_{1A}$ receptor. First, to test the effect of increased F-actin on receptor signaling, we induced depolymerization of F-actin using CD after lovastatin-treatment. In an alternate approach, to explore the contribution of membrane cholesterol in the signaling by the serotonin$_{1A}$ receptor, we acutely replenished membrane cholesterol using the MβCD−cholesterol complex in cells that were earlier subjected to chronic cholesterol depletion. Double-headed arrows (↔) indicate no change from basal level. (B) Values obtained upon quantitation of F-actin in lovastatin-treated (blue bars) and lovastatin/CD-treated cells (yellow bars). To quantify F-actin content, the cellular volume enclosed by the iso-surface (see Figure 4A,B bottom panels) was normalized to the projected area of cells calculated using the software provided with an LSM 510 Meta confocal microscope. Data represent means ± SE of ∼40 different fields from at least three independent experiments [*** corresponds to significant ($p < 0.001$) difference in F-actin content in lovastatin-treated cells relative to untreated cells (gray bars)]. (C) Cholesterol content of lovastatin-treated (blue bars) and lovastatin/CD-treated cells (yellow bars). Values are expressed as absolute cholesterol content and are normalized to total protein content. Data represent means ± SE of three independent experiments [*, **, and *** correspond to significant differences ($p < 0.05$, $p < 0.01$, and $p < 0.001$, respectively) in cholesterol content in lovastatin-treated or lovastatin-/CD-treated cells relative to untreated cells (gray bars)]. Cholesterol content values for lovastatin-treated cells (blue bars) are taken from Figure 1A. (D) Cholesterol content in cells acutely replenished with cholesterol (red bars) subsequent to chronic cholesterol depletion using lovastatin. Acute replenishment of membrane cholesterol was carried out by incubating the cholesterol-depleted cells with a 1 mM cholesterol/10 mM MβCD complex for 10 min in serum-free culture medium. Values are expressed as absolute cholesterol content and are normalized to the total protein content. Cholesterol content values for lovastatin-treated cells (blue bars) are taken from Figure 1A. Data represent means ± SE of three independent experiments [* and *** correspond to significant differences ($p < 0.05$ and $p < 0.001$, respectively) in cholesterol content in lovastatin-treated cells relative to untreated cells (gray bars)]. (E) Values obtained upon quantitation of F-actin in lovastatin-treated (blue bars) and cholesterol-replenished cells (red bars). F-actin content was quantified as described in (B). Data represent means ± SE of ∼40 different fields from at least three independent experiments [*** corresponds to a significant ($p < 0.001$) difference in F-actin content in lovastatin-treated cells relative to untreated cells (gray bars)]. See Methods for more details.

cholesterol replenishment. This prompted us to speculate that signaling by the serotonin$_{1A}$ receptor could be regulated by other factors, as well. Next, we probed the role of the actin cytoskeleton in the signaling carried out by the serotonin$_{1A}$ receptor. As described above, we carried out destabilization of actin cytoskeleton in cholesterol-depleted cells that had higher levels of F-actin. Figure 6A shows that destabilization of the actin cytoskeleton could restore the signaling ability of the serotonin$_{1A}$ receptor (yellow bars), albeit partially, relative to untreated cells (gray bar). As shown in the figure, upon treatment of cholesterol-depleted cells with CD, reductions in cAMP content were restored to 78, 55, and 40%, respectively.

https://doi.org/10.1021/acschemneuro.3c00472
ACS Chem. Neurosci. 2023, 14, 3855−3868

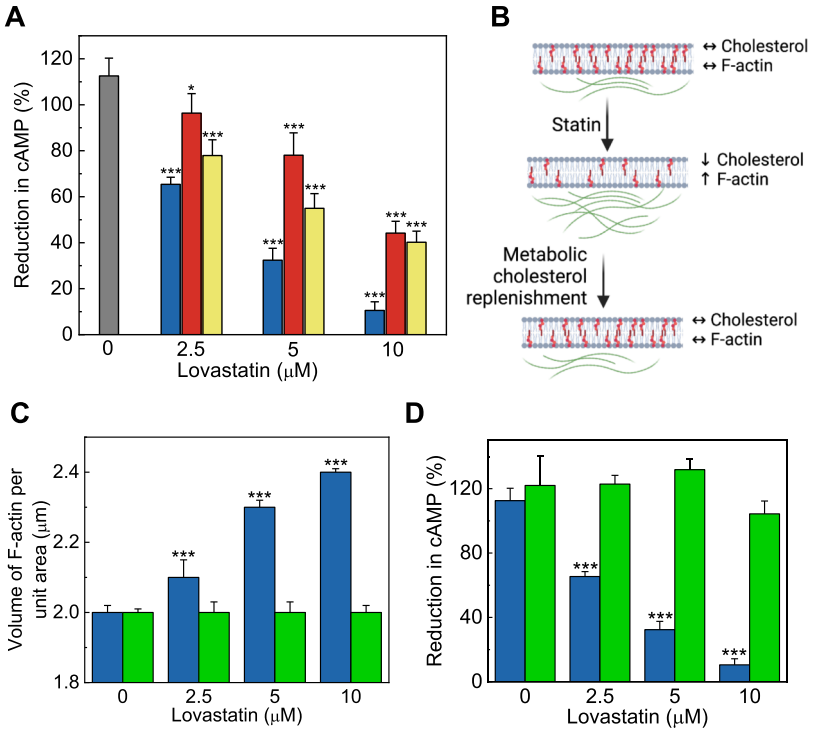

Figure 6. (A) Reduction in serotonin$_{1A}$ receptor signaling upon chronic cholesterol depletion could be rescued via multiple pathways. The relative reduction in cAMP content (a measure of cellular signaling) by the human serotonin$_{1A}$ receptor in lovastatin-treated cells (blue) upon acute cholesterol replenishment (red) and actin cytoskeleton-destabilized (yellow) conditions. Data are normalized to cAMP levels in the presence of 50 μM IBMX/10 μM forskolin (forskolin-stimulated) for each condition. Data for cAMP content for lovastatin-treated cells are taken from Figure 3E. Data represent means ± SE of at least three independent experiments [*** and * correspond to significant ($p < 0.001$ and $p < 0.05$, respectively) differences in cAMP content for lovastatin-treated (blue bars) or cholesterol-replenished (red bars) or lovastatin/CD-treated (yellow bars) cells relative to control cells (gray bars)]. (B) Schematic representation of metabolic replenishment of membrane cholesterol in cells subjected to chronic cholesterol depletion by lovastatin. Metabolic replenishment of cholesterol (shown in red) restores cholesterol level and F-actin (shown as green meshwork underlying the membrane) content similar to control cells (prior to lovastatin treatment). Cholesterol was metabolically replenished in lovastatin-treated cells by incubating cells with complete medium in the absence of lovastatin. Double-headed arrows (↔) indicate no change from basal level. (C) Values obtained upon quantitation of F-actin in cholesterol-depleted (blue) and cholesterol-replenished cells (green). Cellular F-actin was quantified as described in Figures 4 and 5B. Data for F-actin content in lovastatin-treated cells are taken from Figure 5B. Data represent means ± SE of ∼30 different fields from at least three independent experiments [*** corresponds to a significant ($p < 0.001$) difference in F-actin content in lovastatin-treated cells relative to untreated cells]. (D) Chronic cholesterol depletion induced reduction in signaling by the serotonin$_{1A}$ receptor is reversible in nature. The relative reduction in forskolin-stimulated levels of cAMP by the human serotonin$_{1A}$ receptor upon activation by 10 μM serotonin in cholesterol-depleted (blue) and cholesterol-replenished (green) cells. Data are normalized to cAMP levels in the presence of 50 μM IBMX/10 μM forskolin (forskolin-stimulated) for each condition. The data of cAMP content for lovastatin-treated cells are taken from Figure 3E. Data represent means ± SE of at least three independent experiments (*** corresponds to a significant ($p < 0.001$) difference in cAMP content under serotonin-treated condition for cells treated with lovastatin relative to control cells). See Methods for more details.

These results therefore suggest that the release of constraints on lateral diffusion by actin destabilization allows enhanced signaling through dynamic interaction between the receptor and effectors. In other words, the actin cytoskeleton-induced spatial confinement upon chronic cholesterol depletion plays an important role in the regulation of signal transduction by the receptor.

Chronic Cholesterol Replenishment Leads to Complete Recovery of Signaling by the Serotonin$_{1A}$ Receptor. To further establish the role of reduced membrane cholesterol and the effective increase in F-actin content in signaling by the serotonin$_{1A}$ receptor, we metabolically replenished membrane cholesterol in cells subjected to chronic cholesterol depletion by lovastatin (Figure 6B). We incubated lovastatin-treated cells in complete culture medium after washing off the lovastatin-containing medium. As shown in Figures 2C and 6C, metabolic replenishment of cholesterol restored cholesterol levels and F-actin content, respectively, in lovastatin-treated cells to control levels. We then monitored the effect of metabolic cholesterol replenishment on signaling by the serotonin$_{1A}$ receptor by measuring the serotonin-induced reduction in cellular cAMP content. Figure 6D shows that metabolic replenishment of membrane cholesterol completely restored signaling by the serotonin$_{1A}$ receptor. This is in contrast to the results obtained using acute cholesterol replenishment, where we observed a partial recovery of signaling by the serotonin$_{1A}$ receptor (see red bars in Figure 6A). Taken together, our results comprehensively demonstrate that actin cytoskeleton-induced spatial confinement plays a crucial role in regulation of signal transduction by GPCRs.

DISCUSSION

The sensitivity of GPCRs to membrane cholesterol constitutes an exciting and emerging area of research in contemporary GPCR biology.[62−72] According to current estimate, the

https://doi.org/10.1021/acschemneuro.3c00472
ACS Chem. Neurosci. 2023, 14, 3855−3868

function of >50 GPCRs has been shown to be dependent on membrane cholesterol.[72] Previous work from our laboratory has shown that the human serotonin$_{1A}$ receptor exhibits sensitivity toward membrane cholesterol in terms of its oligomerization, dynamics, function, trafficking, and endocytosis.[48−50,73−82] Such cholesterol-dependence of GPCR activity is often correlated either to direct interaction of cholesterol with the receptor through specific cholesterol binding motifs, or to the ability of cholesterol to modulate physical properties in the receptor microenvironment, or a combination of both these effects.[59,83] In this context, we recently showed that a lysine residue (K101) in the cholesterol recognition/interaction amino acid consensus (CRAC) motif in a transmembrane helix of the serotonin$_{1A}$ receptor acts as a sensor of altered membrane cholesterol levels.[58]

A popular approach to explore cholesterol-sensitivity of GPCRs has been depletion of membrane cholesterol, followed by monitoring GPCR function. This is achieved by acute (using carriers such as MβCD) or chronic depletion using inhibitors of cellular cholesterol biosynthesis, such as statins. Interestingly, in addition to reduction in membrane cholesterol content, depletion of membrane cholesterol by statins often involves complex global cellular responses,[84−87] even cell cycle arrest,[88,89] that could complicate the interpretation of functional readouts. In this context, we recently showed that cholesterol depletion using lovastatin leads to extensive polymerization of actin cytoskeleton in a dose-dependent manner.[37] As a consequence of actin polymerization in cholesterol-depleted cells, the serotonin$_{1A}$ receptor experiences dynamic confinement in the plasma membrane and shows reduced lateral mobility (diffusion).[38] With an overall goal of exploring the functional consequence of altered receptor dynamics due to cholesterol depletion by statin, in this work, we probed the role of the actin cytoskeleton in signaling by the serotonin$_{1A}$ receptor. Our results show that cellular signaling by the serotonin$_{1A}$ receptor is fine-tuned by the actin cytoskeleton in a cholesterol-dependent fashion. Importantly, these results demonstrate that whereas actin polymerization acts as a negative regulator of cAMP signaling, cholesterol could act as a positive modulator. We believe that such dynamic reorganization of the actin cytoskeleton could represent an important determinant for membrane protein signaling in metabolic disorders such as Smith-Lemli-Opitz syndrome (SLOS)[90] that are due to defects in cholesterol biosynthesis pathways. It is worthwhile mentioning here that although it has been earlier reported that statins could inhibit GPCR signaling,[91] reorganization of actin cytoskeleton has never been proposed as an underlying mechanism. It is therefore prudent to exercise caution before attributing the cholesterol dependence of membrane protein dynamics and function to mere cholesterol content.

Interestingly, the observed decrease in signaling (Figure 3E) of the serotonin$_{1A}$ receptor upon chronic cholesterol depletion in CHO-K1 cells is different from our earlier results where we reported that acute cholesterol depletion had no appreciable effect on the downstream signaling response.[74] Notably, it is known that the consequence of membrane cholesterol depletion often depends on the actual time scale (acute or chronic) of the process, although the molecular mechanism underlying this difference remains elusive.[47] Whereas the absolute cholesterol content in the membrane could be similar, the finer mechanistic framework associated with each of these processes could be distinct. Acute cholesterol depletion using cyclodextrin-type carriers is known to be a multiphasic process, characterized by differential efficiency of extracting cholesterol from various membrane domains.[92−94] Although acute cholesterol depletion in model membranes has been reported to result in loss of cholesterol preferentially from liquid-disordered (fluid) regions,[95,96] MβCD shows no preference for any specific domain in cell membranes.[97] Chronic cholesterol depletion using biosynthetic inhibitors reduces the cellular synthesis of cholesterol prior to its localization in various membrane domains. In addition, statin treatment involves multiple pleiotropic effects at the global cellular level including cell cycle arrest, induction of autophagy, and inhibition of isoprenylation of small G-proteins.[84,85,88] Many of these cholesterol-independent side-effects of statin are mediated by inhibition of biosynthesis of isoprenoids that are post-translationally attached to crucial intracellular signaling molecules. Interestingly, statins could partition into membranes and induce changes in membrane physical properties (such as membrane order)[86,87] that could affect conformational plasticity of the receptor that is necessary for its function. We therefore believe that the actual method of cholesterol depletion is a critical factor that must be taken into account while interpreting data for complex cellular readouts such as GPCR signaling.

As discussed above, our results show that the sensitivity in cellular signaling exhibited by the serotonin$_{1A}$ receptor appears to be mediated by the cellular F-actin content and membrane cholesterol levels, two key players often associated with receptor compartmentalization in the plasma membrane. In this context, by utilizing fluorescence recovery after photobleaching analysis of the serotonin$_{1A}$ receptor, we previously showed that depolymerization of F-actin results in an increase in mobile fraction of the receptor that exhibited a tight correlation with the signaling efficiency by the serotonin$_{1A}$ receptor.[32] This suggests that signaling by the serotonin$_{1A}$ receptor is regulated by receptor mobility, which is altered upon actin destabilization. In a recent work, we measured lateral diffusion of the serotonin$_{1A}$ receptor using single particle tracking (SPT) under actin-destabilized conditions and showed that actin destabilization alters receptor diffusion, which gets manifested as an increase in functional readouts (ligand binding and cAMP signaling) of the receptor.[35] Notably, previous SPT measurements of neurokinin-1 receptor have further reinforced the proposal of actin cytoskeleton-dependent dynamics of GPCRs, in which receptor confinement strongly correlated to a significant decrease of the receptor canonical signaling pathway.[98] As discussed above, lateral mobility (diffusion) is required to bring together the reacting partners spatially in proximity to form a functional signaling complex. Keeping in mind that G-proteins and other effectors of GPCR signaling (e.g., adenylyl cyclase) are membrane-anchored/bound proteins, it is possible that the observed reduction in serotonin$_{1A}$ receptor signaling could be partly contributed by the reduced lateral mobility of the effectors. Our results described in this work, along with our previous observations, therefore demonstrate the interdependence of membrane protein dynamics with signaling.[27]

Statins are reported to cross the blood−brain barrier based on their lipophilicity.[99−102] In this context, it has been reported that symptoms of anxiety and depression are more frequent in humans upon long-term statin administration,[103−105] and cortical cholesterol level was found to be lower in mood disorders.[106] Keeping in mind the important role of the

https://doi.org/10.1021/acschemneuro.3c00472
ACS Chem. Neurosci. 2023, 14, 3855−3868

serotonin$_{1A}$ receptor in neurological function, on a broader perspective, our results assume significance in understanding the modulatory role of the membrane environment in the organization and function of neurotransmitter GPCRs. We believe that these novel results could have potential significance in the context of signaling by GPCRs, in general, and in the understanding of modulation of signaling by GPCR-cytoskeleton interactions in response to chronic cholesterol depletion, in particular. From a broader and cautionary perspective, we conclude that in analyses of the modulatory role of the membrane environment on the function of membrane proteins, it is prudent to include the actin cytoskeleton as a crucial player".

METHODS

Materials. BSA, cholesterol, CD, DMPC, DMSO, EDTA, forskolin, gentamycin sulfate, Geneticin (G 418), IBMX, MβCD, $CaCl_2$, $MgCl_2$, $MnCl_2$, $NaHCO_3$, phenylmethylsulfonyl fluoride (PMSF), penicillin, poly-L-lysine, serotonin, sodium azide, streptomycin, Triton X-100, and Tris were purchased from Sigma (St. Louis, MO). Alexa Fluor 546 phalloidin and Amplex Red cholesterol assay kit were from Molecular Probes/Invitrogen (Eugene, OR). DMEM/F-12 [Dulbecco's modified Eagle medium: nutrient mixture F-12 (Ham) (1:1)] and fetal calf serum (FCS) were obtained from Invitrogen Life Technologies (Grand Island, NY). [^{3}H]8-OH-DPAT (8-hydroxy-2(di-*N*-propylamino)tetralin, specific activity of 141 Ci/mmol) was obtained from MP Biomedicals (Santa Ana, CA). GF/B glass microfiber filters were from Whatman International (Kent, UK). The HTRF cAMP-Gi assay kit was purchased from CisBio Bioassays (Codolet, France). Bicinchoninic acid (BCA) reagent for protein estimation was from Pierce (Rockford, IL). Lovastatin was obtained from Calbiochem (San Diego, CA). Vectashield Antifade Mounting Medium was obtained from Vector Laboratories (Burlingame, CA). 1-Palmitoyl-2-oleoyl-*sn*-glycero-3-phosphocholine (POPC), 1-palmitoyl-2-oleoyl-*sn*-glycero-3-phosphoglycerol (POPG), 1-palmitoyl-2-oleoyl-*sn*-glycero-3-phosphoethanolamine (POPE), and porcine brain sphingomyelin lipids were obtained from Avanti Polar Lipids (Alabaster, AL). All other chemicals used were of the highest available purity. Purified water through a Millipore (Bedford, MA) Milli-Q system was used for all experiments.

Cell Culture and Treatments. CHO-K1 cells expressing the human serotonin$_{1A}$ receptor tagged to EYFP at the C-terminal (CHO-K1-5HT$_{1A}$R-EYFP)[51] were maintained in DMEM/F-12 (1:1) supplemented with 2.4 g/L of sodium bicarbonate, 10% FCS, 60 μg/mL penicillin, 50 μg/mL streptomycin, 50 μg/mL gentamycin sulfate, and 200 μg/mL Geneticin (complete DMEM/F-12) in a humidified atmosphere with 5% CO_2 at 37 °C. CHO-K1 cells without the serotonin$_{1A}$ receptor were maintained in complete DMEM/F-12 without Geneticin. The stock solution of lovastatin was prepared as described previously,[37] added to cells grown for 24 h (final concentration of lovastatin was 2.5−10 μM), and incubated in complete DMEM/F-12 for 48 h in a humidified atmosphere with 5% CO_2 at 37 °C. For CD treatment, stock solution of 2 mM CD was prepared in DMSO, and further concentrations were prepared upon dilution of the stock in buffer A (PBS containing 1 mM $CaCl_2$ and 0.5 mM $MgCl_2$). After 48 h of treatment with lovastatin, cells were washed once with PBS and treated with 0.5 μM CD for 10 min in a humidified atmosphere with 5% CO_2 at 37 °C.

Replenishment of Membrane Cholesterol. Metabolic replenishment of cholesterol was carried out by incubating cells in lovastatin-free medium. For this, after treatment with lovastatin for 48 h, cells were washed once with PBS and grown in complete DMEM/F-12 medium for 24 h in a humidified atmosphere with 5% CO_2 at 37 °C. Cholesterol-depleted cells were acutely replenished with cholesterol using the cholesterol−MβCD complex. The complex was prepared by dissolving the required amount of cholesterol and MβCD in a ratio of 1:10 (mol/mol) in water with constant shaking at room temperature (~23 °C). Stock solution of the complex (containing 2 mM cholesterol:20 mM MβCD) was freshly prepared before each experiment. Cholesterol replenishment was carried out by incubating the lovastatin-treated cells with 1 mM of the cholesterol/10 mM MβCD complex for 10 min in serum-free DMEM/F-12 medium in a humidified atmosphere with 5% CO_2 at 37 °C followed by a wash with PBS.

Estimation of Cellular Cholesterol Content. Cell monolayers were washed twice with PBS after each treatment. Cholesterol was estimated from cell lysates using the Amplex Red cholesterol assay kit[107] as described previously.[37] Cholesterol values were normalized to total protein levels estimated using BCA assay.[108]

Estimation of Phospholipid Content. Concentrations of phospholipids were estimated by digestion with perchloric acid[109] using Na_2HPO_4 as standard. We used DMPC as an internal standard to assess lipid digestion. Samples digested without perchloric acid showed negligible readings. Phospholipid values were normalized to the total protein content in cell membranes.

F-Actin Labeling of CHO-K1 Cells. F-actin labeling and quantitation in cells were carried out as described previously.[37,38,110] Briefly, cells were plated at a density of ~10^4 on poly-L-lysine-coated 22 mm glass coverslips, and cholesterol modulation was carried out as described above. Cells were washed with buffer A and fixed with ~3.5% (w/v) formaldehyde in buffer A for 10 min at room temperature (~23 °C). Permeabilization of cells was carried out in buffer A with 0.5% Triton X-100 (v/v) for 5 min at room temperature (~23 °C). Stock solutions of Alexa Fluor 546 conjugated phalloidin were prepared in methanol. Cells were washed and stained with Alexa Fluor 546-conjugated phalloidin (final concentration 0.3 μM) in buffer A for 1 h at room temperature (~23 °C) in the dark. After labeling, the coverslips were washed twice with PBS and mounted using Vectashield antifade mounting medium. The edges of the coverslips were sealed with nail enamel and used for imaging.

Fluorescence Microscopy and F-Actin Quantitation. All images were acquired on an inverted Zeiss LSM 510 Meta confocal microscope (Jena, Germany). F-actin was imaged by exciting Alexa Fluor 546 phalloidin at 561 nm and collecting emission from 575 to 630 nm. F-actin quantitation was carried out using a technique previously developed by us.[37,38,110] Briefly, images of *z*-sections were acquired with a 63×/1.4 NA oil immersion objective under 1 airy condition, with a fixed step size of 0.32 μm. Projections of 11 *z*-sections (~3.5 μm from the base of the coverslip into the cell) were generated, and the area of the projected images was determined manually using the software provided with a Zeiss LSM 510 Meta confocal microscope. Iso-surfaces (defined as contours made upon joining voxels of equal fluorescence intensity) were generated from *z*-sections corresponding to each projected image by using Imaris 8.4.0 software (Bitplane AG, Zurich, Switzerland). Iso-surfaces were obtained upon fluorescence intensity thresholding of *z*-sections followed by applying a Gaussian filter. The estimated volumes enclosed by iso-surfaces were normalized to the projected area of cells for a given field.

Flow Cytometric Analysis of the Receptor Expression Level. CHO-K1-5HT$_{1A}$R-EYFP cells were collected in PBS containing 0.25 mM EDTA, washed in serum-free DMEM/F-12 medium, and then resuspended in PBS containing 2% (v/v) FCS. Populations of cells associated with the serotonin$_{1A}$ receptor under control and lovastatin-treated conditions were quantified using a Gallios flow cytometer (Beckman Coulter, Brea, CA), and data were analyzed using Kaluza analysis software version 2.1 (Beckman Coulter, Brea, CA). Excitation was set at 488 nm, emission was collected using a 525/40 bandpass filter, and 10,000 cells were estimated for each condition. Fluorescence from cells expressing the serotonin$_{1A}$ receptor without the EYFP tag was used to gate EFYP-positive cells.

Radioligand Binding Assay in Live Cells. CHO-K1-5HT$_{1A}$R-EYFP cells were detached from culture flasks in PBS containing 0.25 mM EDTA after lovastatin treatment. Cells were spun at 500*g* for 5 min and resuspended in serum-free DMEM/F-12 medium for counting using a hemocytometer. Cells (~10^6) in serum-free DMEM/F-12 medium were incubated at ~25 °C for 15 min in the presence of 1 nM [^{3}H]8-OH-DPAT (specific agonist). Nonspecific

https://doi.org/10.1021/acschemneuro.3c00472
ACS Chem. Neurosci. 2023, 14, 3855−3868

binding was obtained by performing the assay in the presence of 10 μM unlabeled serotonin. The binding reaction was terminated by rapid filtration under vacuum in a Millipore multiport filtration apparatus through Whatman GF/B filters (1.0 μm pore size) which were presoaked in 0.5% (w/v) polyethylenimine for 3 h.[111] Following this, filters were washed three times with 5 mL of cold water (~4 °C) and dried, and the retained radioactivity was measured in a Packard Tri-Carb 2900 liquid scintillation counter (PerkinElmer, Waltham, MA) using 5 mL of scintillation fluid. To rule out any effect of receptor endocytosis during the time of incubation with radiolabeled agonist, we pretreated the cells with 10 mM sodium azide (inhibitor of ATP synthesis) for 30 min before radioligand binding experiments.

Saturation Binding Assay. Saturation binding assays were carried out to estimate binding parameters in control and lovastatin-treated cells. Assays were carried out with increasing concentrations of the radiolabeled agonist [^{3}H]8-OH-DPAT (0.1−7.5 nM) in intact cells. Nonspecific binding was determined by performing the assay in the presence of 10 μM unlabeled serotonin. Ligand binding assays were carried out at ~25 °C with ~10^6 cells for each ligand concentration. The concentration of bound radioligand (RL_{bound}) was determined using the equation[35]

$$RL_{bound} = 10^{-9} \times B/(V \times SA \times 2220)\ M \quad (1)$$

where B is the bound radioactivity in disintegrations per minute (dpm), V is the assay volume in mL, and SA is the specific activity of the radioligand. Saturation binding data could be fitted best to a one-site ligand binding equation given below

$$RL_{bound} = B_{max}x/(K_d + x) \quad (2)$$

where x is the total ligand concentration, K_d is the dissociation constant, and B_{max} is the number of maximum binding sites. Values of K_d and B_{max} were obtained by nonlinear regression analysis of binding data using GraphPad Prism software, version 4.0 (San Diego, CA).

Cellular Signaling Assay. Cellular signaling assays to estimate cAMP levels were carried out as described previously.[35,58] CHO-K1-$5HT_{1A}$R-EYFP cells were plated at a density of ~10^5 cells in poly-L-lysine coated 6-well plates and grown in complete medium in a humidified incubator with 5% CO_2 at 37 °C. After treatment with lovastatin, cells were treated with 50 μM IBMX (basal), 50 μM IBMX/10 μM forskolin (forskolin-stimulated), and 50 μM IBMX/10 μM forskolin/10 μM serotonin (agonist treatment) and incubated for 30 min at 37 °C. After discarding media, cells were washed with PBS and lifted using a cell scraper. Cells were counted using a hemocytometer and added at 6000 cells/well to a low-volume HTRF 96-well plate (CisBio Bioassays, Codolet, France). The ability of the serotonin$_{1A}$ receptor to inhibit the forskolin-stimulated increase in cAMP levels was assessed using the FRET-based HTRF cAMP-Gi assay kit (CisBio Bioassays, Codolet, France). Fluorescence was measured at 620 nm (cAMP-cryptate donor emission) and 655 nm (anti-cAMP-d2 acceptor emission) upon excitation of the donor at 320 nm using an EnSpire Multimode Plate Reader (PerkinElmer, Waltham, MA). cAMP levels were calculated as a ratio of the acceptor and donor emission. Values for serotonin-induced cAMP reduction were normalized and expressed as a percentage of the values obtained for only forskolin-treated cells.

Thin-Layer Chromatography. Lipid extraction from cell membranes obtained from control and cells treated with increasing concentration of lovastatin was carried out according to the Bligh and Dyer method.[112] Lipid extracts from ~1 mg of protein were dried under a stream of argon at ~40 °C, and the dried lipids were dissolved in chloroform/methanol (1:1, v/v). Lipids were resolved on precoated silica gel TLC plates using chloroform/methanol/water (65:25:4, v/v/v) as the solvent system.[113] Cholesterol, POPE, POPG, POPC, and sphingomyelin standards were run to identify the corresponding bands in lipid extracts obtained from control and lovastatin-treated cells. The separated lipids were visualized by charring with a solution containing 8% (v/v) phosphoric acid and 10% (w/v) cupric sulfate at ~150 °C.[114]

Statistical Analysis. Significance levels were estimated using Student's two-tailed unpaired t-test using GraphPad Prism software, version 4.0 (San Diego, CA). Plots were generated using Microcal Origin version 9.7 (OriginLab Corporation, Northampton, MA).

■ ASSOCIATED CONTENT

Supporting Information

The Supporting Information is available free of charge at https://pubs.acs.org/doi/10.1021/acschemneuro.3c00472.

Membrane phospholipid content upon lovastatin treatment (PDF)

■ AUTHOR INFORMATION

Corresponding Author

Amitabha Chattopadhyay − *CSIR-Centre for Cellular and Molecular Biology, Hyderabad 500 007, India; Academy of Scientific and Innovative Research, Ghaziabad 201 002, India;* orcid.org/0000-0002-2618-2565; Phone: +91-40-2719-2578; Email: amit@ccmb.res.in

Author

Parijat Sarkar − *CSIR-Centre for Cellular and Molecular Biology, Hyderabad 500 007, India;* Present Address: Department of Biochemistry, Stanford University, School of Medicine, Stanford, CA 94305, USA

Complete contact information is available at: https://pubs.acs.org/10.1021/acschemneuro.3c00472

Author Contributions

P.S. performed all experiments and analyzed data; P.S. and A.C. designed the experiments and the project framework; P.S. and A.C. wrote the manuscript. A.C. conceptualized the project, edited the manuscript in its final version, organized access to research facilities and funding, and provided overall supervision and mentoring.

Notes

The authors declare no competing financial interest.

■ ACKNOWLEDGMENTS

A.C. gratefully acknowledges support from CSIR Bhatnagar Fellowship. P.S. was supported as a Senior Project Associate by a CSIR Focused Basic Research (FBR) Grant to A.C. (MLP 0146). We thank Gunda Srinivas for help with acquiring flow cytometric data. We gratefully acknowledge members of the Chattopadhyay laboratory, G. Aditya Kumar (University of Michigan Medical School, Ann Arbor, MI) and Bhagyashree Rao (The Francis Crick Institute, London, UK) for their comments and suggestions.

■ ABBREVIATIONS

BSA, bovine serum albumin; BCA, bicinchoninic acid; CD, cytochalasin D; CHO, Chinese hamster ovary; DMPC, 1,2-dimyristoyl-*sn*-glycero-3-phosphocholine; DMSO, dimethyl sulfoxide; EDTA, ethylenediaminetetraacetic acid; EYFP, enhanced yellow fluorescent protein; GPCR, G protein-coupled receptor; MβCD, methyl-β-cyclodextrin; PBS, phosphate buffered saline; cAMP, adenosine 3′,5′-cyclic monophosphate; FRET, fluorescence resonance energy transfer; IBMX, 3-isobutyl-1-methylxanthine; 8-OH-DPAT, 8-hydroxy-2(di-*N*-propylamino)tetralin

https://doi.org/10.1021/acschemneuro.3c00472
ACS Chem. Neurosci. 2023, 14, 3855−3868

REFERENCES

(1) Chattopadhyay, A. GPCRs: lipid-dependent membrane receptors that act as drug targets. *Adv. Biol.* **2014**, *2014*, 1−12.
(2) Sakmar, T. P. Introduction: G-protein coupled receptors. *Chem. Rev.* **2017**, *117*, 1−3.
(3) Wootten, D.; Christopoulos, A.; Marti-Solano, M.; Babu, M. M.; Sexton, P. M. Mechanisms of signalling and biased agonism in G protein-coupled receptors. *Nat. Rev. Mol. Cell Biol.* **2018**, *19*, 638−653.
(4) Erlandson, S. C.; McMahon, C.; Kruse, A. C. Structural basis for G protein-coupled receptor signaling. *Annu. Rev. Biophys.* **2018**, *47*, 1−18.
(5) Weis, W. I.; Kobilka, B. K. The molecular basis of G protein-coupled receptor activation. *Annu. Rev. Biochem.* **2018**, *87*, 897−919.
(6) Wingler, L. M.; Lefkowitz, R. J. Conformational basis of G protein-coupled receptor signaling versatility. *Trends Cell Biol.* **2020**, *30*, 736−747.
(7) Jacobson, K. A. New paradigms in GPCR drug discovery. *Biochem. Pharmacol.* **2015**, *98*, 541−555.
(8) Sriram, K.; Insel, P. A. G protein-coupled receptors as targets for approved drugs: How many targets and how many drugs? *Mol. Pharmacol.* **2018**, *93*, 251−258.
(9) Chan, H. S.; Li, Y.; Dahoun, T.; Vogel, H.; Yuan, S. New binding sites, new opportunities for GPCR drug discovery. *Trends Biochem. Sci.* **2019**, *44*, 312−330.
(10) Yang, D.; Zhou, Q.; Labroska, V.; Qin, S.; Darbalaei, S.; Wu, Y.; Yuliantie, E.; Xie, L.; Tao, H.; Cheng, J.; et al. G protein-coupled receptors: structure- and function-based drug discovery. *Signal Transduction Targeted Ther.* **2021**, *6*, 7.
(11) Lobingier, B. T.; von Zastrow, M. When trafficking and signaling mix: how subcellular location shapes G protein-coupled receptor activation of heterotrimeric G proteins. *Traffic* **2019**, *20*, 130−136.
(12) Crilly, S. E.; Puthenveedu, M. A. Compartmentalized GPCR signaling from intracellular membranes. *J. Membr. Biol.* **2021**, *254*, 259−271.
(13) Calebrio, D. Signalling by G protein-coupled receptors: why space and time matter. *Eur. J. Endocrinol.* **2021**, *184*, R41−R49.
(14) Kumar, G. A.; Puthenveedu, M. A. Diversity and specificity in location-based signaling outputs of neuronal GPCRs. *Curr. Opin. Neurobiol.* **2022**, *76*, 102601.
(15) Ribeiro-Oliveira, R.; Vojtek, M.; Gonçalves-Monteiro, S.; Vieira-Rocha, M. S.; Sousa, J. B.; Gonçalves, J.; Diniz, C. Nuclear G-protein-coupled receptors as putative novel pharmacological targets. *Drug Discovery Today* **2019**, *24*, 2192−2201.
(16) Fasciani, I.; Carli, M.; Petragnano, F.; Colaianni, F.; Aloisi, G.; Maggio, R.; Scarselli, M.; Rossi, M. GPCRs in intracellular compartments: new targets for drug discovery. *Biomolecules* **2022**, *12*, 1343.
(17) Pucadyil, T. J.; Kalipatnapu, S.; Chattopadhyay, A. The serotonin$_{1A}$ receptor: A representative member of the serotonin receptor family. *Cell. Mol. Neurobiol.* **2005**, *25*, 553−580.
(18) Kalipatnapu, S.; Chattopadhyay, A. Membrane organization and function of the serotonin$_{1A}$ receptor. *Cell. Mol. Neurobiol.* **2007**, *27*, 1097−1116.
(19) Müller, C. P.; Carey, R. J.; Huston, J. P.; De Souza Silva, M. A. Serotonin and psychostimulant addiction: Focus on 5-HT$_{1A}$ receptors. *Prog. Neurobiol.* **2007**, *81*, 133−178.
(20) Glikmann-Johnston, Y.; Saling, M. M.; Reutens, D. C.; Stout, J. C. Hippocampal 5-HT$_{1A}$ receptor and spatial learning and memory. *Front. Pharmacol* **2015**, *6*, 289.
(21) Sarkar, P.; Kumar, G. A.; Pal, S.; Chattopadhyay, A. Biophysics of Serotonin and the Serotonin$_{1A}$ Receptor: Fluorescence and Dynamics. In *Serotonin: The Mediator That Spans Evolution*; Pilowsky, P., Ed.; Elsevier: Amsterdam, 2018; pp 3−22.
(22) Sarkar, P.; Mozumder, S.; Bej, A.; Mukherjee, S.; Sengupta, J.; Chattopadhyay, A. Structure, dynamics and lipid interactions of serotonin receptors: Excitements and challenges. *Biophys. Rev.* **2021**, *13*, 101−122.
(23) Lacivita, E.; Leopoldo, M.; Berardi, F.; Perrone, R. 5-HT$_{1A}$ receptor, an old target for new therapeutic agents. *Curr. Top. Med. Chem.* **2008**, *8*, 1024−1034.
(24) Fiorino, F.; Severino, B.; Magli, E.; Ciano, A.; Caliendo, G.; Santagada, V.; Frecentese, F.; Perissutti, E. 5-HT$_{1A}$ receptor: an old target as a new attractive tool in drug discovery from central nervous system to cancer. *J. Med. Chem.* **2014**, *57*, 4407−4426.
(25) Cuatrecasas, P. Membrane receptors. *Annu. Rev. Biochem.* **1974**, *43*, 169−214.
(26) Jacobs, S.; Cuatrecasas, P. The mobile receptor hypothesis for cell membrane receptor action. *Trends Biochem. Sci.* **1977**, *2*, 280−282.
(27) Sarkar, P.; Chattopadhyay, A. Insights into cellular signaling from membrane dynamics. *Arch. Biochem. Biophys.* **2021**, *701*, 108794.
(28) Jacobson, K.; Mouritsen, O. G.; Anderson, R. G. W. Lipid rafts: at a crossroad between cell biology and physics. *Nat. Cell Biol.* **2007**, *9*, 7−14.
(29) Latorraca, N. R.; Venkatakrishnan, A. J.; Dror, R. O. GPCR dynamics: Structures in motion. *Chem. Rev.* **2017**, *117*, 139−155.
(30) Jans, D. A.; Peters, R.; Jans, P.; Fahrenholz, F. Vasopressin V$_2$-receptor mobile fraction and ligand-dependent adenylate cyclase activity are directly correlated in LLC-PK1 renal epithelial cells. *J. Cell Biol.* **1991**, *114*, 53−60.
(31) Calvert, P. D.; Govardovskii, V. I.; Krasnoperova, N.; Anderson, R. E.; Lem, J.; Makino, C. L. Membrane protein diffusion sets the speed of rod phototransduction. *Nature* **2001**, *411*, 90−94.
(32) Ganguly, S.; Pucadyil, T. J.; Chattopadhyay, A. Actin cytoskeleton-dependent dynamics of the human serotonin$_{1A}$ receptor correlates with receptor signaling. *Biophys. J.* **2008**, *95*, 451−463.
(33) Kusumi, A.; Murakoshi, H.; Murase, K.; Fujiwara, T. Single-molecule Imaging of Diffusion, Recruitment, and Activation of Signaling Molecules in Living Cells. In *Biophysical Aspects of Transmembrane Signaling*; Damjanovich, S., Ed.; *Springer Series in Biophysics*; Springer-Verlag: Berlin, 2005; pp 123−152.
(34) Suzuki, K.; Ritchie, K.; Kajikawa, E.; Fujiwara, T.; Kusumi, A. Rapid hop diffusion of a G-protein-coupled receptor in the plasma membrane as revealed by single-molecule techniques. *Biophys. J.* **2005**, *88*, 3659−3680.
(35) Shrivastava, S.; Sarkar, P.; Preira, P.; Salomé, L.; Chattopadhyay, A. Role of actin cytoskeleton in dynamics and function of the serotonin$_{1A}$ receptor. *Biophys. J.* **2020**, *118*, 944−956.
(36) Shrivastava, S.; Sarkar, P.; Preira, P.; Salomé, L.; Chattopadhyay, A. Cholesterol-dependent dynamics of the serotonin$_{1A}$ receptor utilizing single particle tracking: analysis of diffusion modes. *J. Phys. Chem. B* **2022**, *126*, 6682−6690.
(37) Sarkar, P.; Kumar, G. A.; Shrivastava, S.; Chattopadhyay, A. Chronic cholesterol depletion increases F-actin levels and induces cytoskeletal reorganization via a dual mechanism. *J. Lipid Res.* **2022**, *63*, 100206.
(38) Sarkar, P.; Chattopadhyay, A. Statin-induced increase in actin polymerization modulates GPCR dynamics and compartmentalization. *Biophys. J.* **2023**, *122*, 1938−1955.
(39) Stossel, T. P. The discovery of statins. *Cell* **2008**, *134*, 903−905.
(40) Endo, A. A historical perspective on the discovery of statins. *Proc. Jpn. Acad., Ser. B* **2010**, *86*, 484−493.
(41) Goldstein, J. L.; Brown, M. S. A century of cholesterol and coronaries: From plaques to genes to statins. *Cell* **2015**, *161*, 161−172.
(42) Greenspan, M. D.; Yudkovitz, J. B.; Lo, C. Y.; Chen, J. S.; Alberts, A. W.; Hunt, V. M.; Chang, M. N.; Yang, S. S.; Thompson, K. L.; Chiang, Y. C. Inhibition of hydroxymethylglutaryl-coenzyme A synthase by L-659,699. *Proc. Natl. Acad. Sci. U.S.A.* **1987**, *84*, 7488−7492.
(43) Istvan, E. S.; Deisenhofer, J. Structural mechanism for statin inhibition of HMG-CoA reductase. *Science* **2001**, *292*, 1160−1164.
(44) Endo, A. A gift from nature: the birth of the statins. *Nat. Med.* **2008**, *14*, 1050−1052.

https://doi.org/10.1021/acschemneuro.3c00472
ACS Chem. Neurosci. 2023, 14, 3855−3868

(45) Kastelein, J. J.; Akdim, F.; Stroes, E. S.; Zwinderman, A. H.; Bots, M. L.; Stalenhoef, A. F.; Visseren, F. L.; Sijbrands, E. J.; Trip, M. D.; Stein, E. A.; Gaudet, D.; Duivenvoorden, R.; Veltri, E. P.; Marais, A. D.; de Groot, E. Simvastatin with or without Ezetimibe in Familial Hypercholesterolemia. *N. Engl. J. Med.* **2008**, *358*, 1431−1443.
(46) Collins, R.; Reith, C.; Emberson, J.; Armitage, J.; Baigent, C.; Blackwell, L.; Blumenthal, R.; Danesh, J.; Smith, G. D.; DeMets, D.; Evans, S.; Law, M.; MacMahon, S.; Martin, S.; Neal, B.; Poulter, N.; Preiss, D.; Ridker, P.; Roberts, I.; Rodgers, A.; Sandercock, P.; Schulz, K.; Sever, P.; Simes, J.; Smeeth, L.; Wald, N.; Yusuf, S.; Peto, R. Interpretation of the evidence for the efficacy and safety of statin therapy. *Lancet* **2016**, *388*, 2532−2561.
(47) Sarkar, P.; Chakraborty, H.; Chattopadhyay, A. Differential membrane dipolar orientation induced by acute and chronic cholesterol depletion. *Sci. Rep.* **2017**, *7*, 4484.
(48) Kumar, G. A.; Chattopadhyay, A. Statin-induced chronic cholesterol depletion switches GPCR endocytosis and trafficking: Insights from the serotonin$_{1A}$ receptor. *ACS Chem. Neurosci.* **2020**, *11*, 453−465.
(49) Kumar, G. A.; Chattopadhyay, A. Membrane cholesterol regulates endocytosis and trafficking of the serotonin$_{1A}$ receptor: Insights from acute cholesterol depletion. *Biochim. Biophys. Acta, Mol. Cell Biol. Lipids* **2021**, *1866*, 158882.
(50) Kumar, G. A.; Chattopadhyay, A. Cholesterol-dependent endocytosis of GPCRs: Implications in pathophysiology and therapeutics. *Biophys. Rev.* **2021**, *13*, 1007−1017.
(51) Pucadyil, T. J.; Kalipatnapu, S.; Harikumar, K. G.; Rangaraj, N.; Karnik, S. S.; Chattopadhyay, A. G-protein-dependent cell surface dynamics of the human serotonin$_{1A}$ receptor tagged to yellow fluorescent protein. *Biochemistry* **2004**, *43*, 15852−15862.
(52) Kumar, G. A.; Sarkar, P.; Jafurulla, M.; Singh, S. P.; Srinivas, G.; Pande, G.; Chattopadhyay, A. Exploring endocytosis and intracellular trafficking of the human serotonin$_{1A}$ receptor. *Biochemistry* **2019**, *58*, 2628−2641.
(53) Raymond, J. R.; Olsen, C. L.; Gettys, T. W. Cell-specific physical and functional coupling of human 5-HT1A receptors to inhibitory G protein .alpha.-subunits and lack of coupling to Gs.alpha. *Biochemistry* **1993**, *32*, 11064−11073.
(54) Raymond, J. R.; Mukhin, Y. V.; Gettys, T. W.; Garnovskaya, M. N. The recombinant 5-HT$_{1A}$ receptor: G protein coupling and signalling pathways. *Br. J. Pharmacol.* **1999**, *127*, 1751−1764.
(55) Giulietti, M.; Vivenzio, V.; Piva, F.; Principato, G.; Bellantuono, C.; Nardi, B. How much do we know about the coupling of G-proteins to serotonin receptors? *Mol. Brain* **2014**, *7*, 49.
(56) Tardieu, J.-L. Selecting a cyclic AMP kit for assaying GPCR target activation. *Nat. Methods* **2008**, *5*, iii−iv.
(57) Ward, R. J.; Pediani, J. D.; Harikumar, K. G.; Miller, L. J.; Milligan, G. Spatial intensity distribution analysis quantifies the extent and regulation of homodimerization of the secretin receptor. *Biochem. J.* **2017**, *474*, 1879−1895.
(58) Kumar, G. A.; Sarkar, P.; Stepniewski, T. M.; Jafurulla, M.; Singh, S. P.; Selent, J.; Chattopadhyay, A. A molecular sensor for cholesterol in the human serotonin$_{1A}$ receptor. *Sci. Adv.* **2021**, *7*, No. eabh2922.
(59) Jafurulla, M.; Kumar, G. A.; Rao, B. D.; Chattopadhyay, A. A critical analysis of molecular mechanisms underlying membrane cholesterol sensitivity of GPCRs. *Cholesterol Modulation of Protein Function*; *Advances in Experimental Medicine and Biology*; Springer, 2019; Vol. *1115*, pp 21−52.
(60) Casella, J. F.; Flanagan, M. D.; Lin, S. Cytochalasin D inhibits actin polymerization and induces depolymerization of actin filaments formed during platelet shape change. *Nature* **1981**, *293*, 302−305.
(61) Schliwa, M. Action of cytochalasin D on cytoskeletal networks. *J. Cell Biol.* **1982**, *92*, 79−91.
(62) Pucadyil, T. J.; Chattopadhyay, A. Role of cholesterol in the function and organization of G protein-coupled receptors. *Prog. Lipid Res.* **2006**, *45*, 295−333.
(63) Paila, Y. D.; Chattopadhyay, A. Membrane cholesterol in the function and organization of G-protein coupled receptors. *Subcell. Biochem.* **2010**, *51*, 439−466.
(64) Oates, J.; Watts, A. Uncovering the intimate relationship between lipids, cholesterol and GPCR activation. *Curr. Opin. Struct. Biol.* **2011**, *21*, 802−807.
(65) Jafurulla, M.; Chattopadhyay, A. Membrane lipids in the function of serotonin and adrenergic receptors. *Curr. Med. Chem.* **2012**, *20*, 47−55.
(66) Sengupta, D.; Chattopadhyay, A. Molecular dynamics simulations of GPCR-cholesterol interaction: An emerging paradigm. *Biochim. Biophys. Acta* **2015**, *1848*, 1775−1782.
(67) Gimpl, G. Interaction of G protein coupled receptors and cholesterol. *Chem. Phys. Lipids* **2016**, *199*, 61−73.
(68) Kiriakidi, S.; Kolocouris, A.; Liapakis, G.; Ikram, S.; Durdagi, S.; Mavromoustakos, T. Effects of cholesterol on GPCR function: insights from computational and experimental studies. *Adv. Exp. Med. Biol.* **2019**, *1135*, 89−103.
(69) Jakubík, J.; El-Fakahany, E. E. Allosteric modulation of GPCRs of class A by cholesterol. *Int. J. Mol. Sci.* **2021**, *22*, 1953.
(70) Sarkar, P.; Chattopadhyay, A. Cholesterol footprint in high-resolution structures of serotonin receptors: where are we now and what does it mean? *Chem. Phys. Lipids* **2021**, *239*, 105120.
(71) Baccouch, R.; Rascol, E.; Stoklosa, K.; Alves, I. D. The role of the lipid environment in the activity of G protein coupled receptors. *Biophys. Chem.* **2022**, *285*, 106794.
(72) Sarkar, P.; Chattopadhyay, A. Cholesterol in GPCR structures: Prevalence and relevance. *J. Membr. Biol.* **2022**, *255*, 99−106.
(73) Pucadyil, T. J.; Chattopadhyay, A. Cholesterol modulates ligand binding and G-protein coupling to serotonin$_{1A}$ receptors from bovine hippocampus. *Biochim. Biophys. Acta* **2004**, *1663*, 188−200.
(74) Pucadyil, T. J.; Chattopadhyay, A. Cholesterol depletion induces dynamic confinement of the G-protein coupled serotonin$_{1A}$ receptor in the plasma membrane of living cells. *Biochim. Biophys. Acta* **2007**, *1768*, 655−668.
(75) Paila, Y. D.; Murty, M. R. V. S.; Vairamani, M.; Chattopadhyay, A. Signaling by the human serotonin$_{1A}$ receptor is impaired in cellular model of Smith-Lemli-Opitz syndrome. *Biochim. Biophys. Acta* **2008**, *1778*, 1508−1516.
(76) Ganguly, S.; Chattopadhyay, A. Cholesterol depletion mimics the effect of cytoskeletal destabilization on membrane dynamics of the serotonin$_{1A}$ receptor: A zFCS study. *Biophys. J.* **2010**, *99*, 1397−1407.
(77) Shrivastava, S.; Pucadyil, T. J.; Paila, Y. D.; Ganguly, S.; Chattopadhyay, A. Chronic cholesterol depletion using statin impairs the function and dynamics of human serotonin$_{1A}$ receptors. *Biochemistry* **2010**, *49*, 5426−5435.
(78) Ganguly, S.; Clayton, A. H. A.; Chattopadhyay, A. Organization of higher order oligomers of the serotonin$_{1A}$ receptor explored utilizing homo-FRET in live cells. *Biophys. J.* **2011**, *100*, 361−368.
(79) Jafurulla, M.; Rao, B. D.; Sreedevi, S.; Ruysschaert, J.-M.; Covey, D. F.; Chattopadhyay, A. Stereospecific requirement of cholesterol in the function of the serotonin$_{1A}$ receptor. *Biochim. Biophys. Acta* **2014**, *1838*, 158−163.
(80) Sharma, A.; Kumar, G. A.; Chattopadhyay, A. Late endosomal/lysosomal accumulation of a neurotransmitter receptor in a cellular model of Smith-Lemli-Opitz syndrome. *Traffic* **2021**, *22*, 332−344.
(81) Chakraborty, H.; Jafurulla, M.; Clayton, A. H. A.; Chattopadhyay, A. Exploring oligomeric state of the serotonin$_{1A}$ receptor utilizing photobleaching image correlation spectroscopy: Implications for receptor function. *Faraday Discuss.* **2018**, *207*, 409−421.
(82) Sarkar, P.; Jafurulla, M.; Bhowmick, S.; Chattopadhyay, A. Structural stringency and optimal nature of cholesterol requirement in the function of the serotonin$_{1A}$ receptor. *J. Membr. Biol.* **2020**, *253*, 445−457.
(83) Paila, Y. D.; Chattopadhyay, A. The function of G-protein coupled receptors and membrane cholesterol: Specific or general interaction? *Glycoconjugate J.* **2009**, *26*, 711−720.

https://doi.org/10.1021/acschemneuro.3c00472
ACS Chem. Neurosci. 2023, 14, 3855−3868

(84) Cheng, J.; Ohsaki, Y.; Tauchi-Sato, K.; Fujita, A.; Fujimoto, T. Cholesterol depletion induces autophagy. *Biochem. Biophys. Res. Commun.* **2006**, *351*, 246−252.
(85) Tennakoon, M.; Kankanamge, D.; Senarath, K.; Fasih, Z.; Karunarathne, A. Statins Perturb Gβγ Signaling and Cell Behavior in a Gγ Subtype Dependent Manner. *Mol. Pharmacol.* **2019**, *95*, 361−375.
(86) Sahu, S. S.; Sarkar, P.; Shrivastava, S.; Chattopadhyay, A. Differential effects of simvastatin on membrane organization and dynamics in varying phases. *Chem. Phys. Lipids* **2019**, *225*, 104831.
(87) Sariisik, E.; Koçak, M.; Kucuk Baloglu, F.; Severcan, F. Interaction of the cholesterol reducing agent simvastatin with zwitterionic DPPC and charged DPPG phospholipid membranes. *Biochim. Biophys. Acta* **2019**, *1861*, 810−818.
(88) Singh, P.; Saxena, R.; Srinivas, G.; Pande, G.; Chattopadhyay, A. Cholesterol biosynthesis and homeostasis in regulation of the cell cycle. *PLoS One* **2013**, *8*, No. e58833.
(89) Sarkar, P.; Rao, B. D.; Chattopadhyay, A. Cell cycle dependent modulation of membrane dipole potential and neurotransmitter receptor activity: Role of membrane cholesterol. *ACS Chem. Neurosci.* **2020**, *11*, 2890−2899.
(90) Chattopadhyay, A.; Sharma, A. Smith-Lemli-Opitz syndrome: A pathophysiological manifestation of the Bloch hypothesis. *Front. Mol. Biosci.* **2023**, *10*, 1120373.
(91) Harikumar, K. G.; Puri, V.; Singh, R. D.; Hanada, K.; Pagano, R. E.; Miller, L. J. Differential effects of modification of membrane cholesterol and sphingolipids on the conformation, function, and trafficking of the G protein-coupled cholecystokinin receptor. *J. Biol. Chem.* **2005**, *280*, 2176−2185.
(92) Kilsdonk, E. P. C.; Yancey, P. G.; Stoudt, G. W.; Bangerter, F. W.; Johnson, W. J.; Phillips, M. C.; Rothblat, G. H. Cellular cholesterol efflux mediated by cyclodextrins. *J. Biol. Chem.* **1995**, *270*, 17250−17256.
(93) Yancey, P. G.; Rodrigueza, W. V.; Kilsdonk, E. P.; Stoudt, G. W.; Johnson, W. J.; Phillips, M. C.; Rothblat, G. H. Cellular Cholesterol Efflux Mediated by Cyclodextrins. *J. Biol. Chem.* **1996**, *271*, 16026−16034.
(94) Zidovetzki, R.; Levitan, I. Use of cyclodextrins to manipulate plasma membrane cholesterol content: evidence, misconceptions and control strategies. *Biochim. Biophys. Acta* **2007**, *1768*, 1311−1324.
(95) Sanchez, S. A.; Gunther, G.; Tricerri, M. A.; Gratton, E. Methyl-β-cyclodextrins preferentially remove cholesterol from the liquid disordered phase in giant unilamellar vesicles. *J. Membr. Biol.* **2011**, *241*, 1−10.
(96) López, C. A.; de Vries, A. H.; Marrink, S. J. Computational microscopy of cyclodextrin mediated cholesterol extraction from lipid model membranes. *Sci. Rep.* **2013**, *3*, 2071.
(97) Mahammad, S.; Parmryd, I. Cholesterol homeostasis in T cells. Methyl-β-cyclodextrin treatment results in equal loss of cholesterol from Triton X-100 soluble and insoluble fractions. *Biochim. Biophys. Acta* **2008**, *1778*, 1251−1258.
(98) Veya, L.; Piguet, J.; Vogel, H. Single molecule imaging deciphers the relation between mobility and signaling of a prototypical G protein-coupled receptor in living cells. *J. Biol. Chem.* **2015**, *290*, 27723−27735.
(99) Saheki, A.; Terasaki, T.; Tamai, I.; Tsuji, A. *In vivo* and *in vitro* blood-brain barrier transport of 3-hydroxy-3-methylglutaryl coenzyme A (HMG-CoA) reductase inhibitors. *Pharm. Res.* **1994**, *11*, 305−311.
(100) Kirsch, C.; Eckert, G. P.; Koudinov, A. R.; Müller, W. E. Brain cholesterol, statins and Alzheimer's disease. *Pharmacopsychiatry* **2003**, *36*, 113−119.
(101) Wood, W. G.; Eckert, G. P.; Igbavboa, U.; Müller, W. E. Statins and neuroprotection. A prescription to move the field forward. *Ann. N.Y. Acad. Sci.* **2010**, *1199*, 69−76.
(102) Sierra, S.; Ramos, M. C.; Molina, P.; Esteo, C.; Vázquez, J. A.; Burgos, J. S. Statins as neuroprotectants: a comparative *in vitro* study of lipophilicity, blood-brain-barrier penetration, lowering of brain cholesterol, and decrease of neuron cell death. *J. Alzheimer's Dis.* **2011**, *23*, 307−318.
(103) Zureik, M.; Courbon, D.; Ducimetiere, P. Serum cholesterol concentration and death from suicide in men: Paris prospective study I. *Br. Med. J.* **1996**, *313*, 649−651.
(104) Golomb, B. A.; Criqui, M. H.; White, H.; Dimsdale, J. E. Conceptual foundations of the UCSD Statin Study: a randomized controlled trial assessing the impact of statins on cognition, behavior, and biochemistry. *Arch. Intern. Med.* **2004**, *164*, 153−162.
(105) Papakostas, G. I.; Öngür, D.; Iosifescu, D. V.; Mischoulon, D.; Fava, M. Cholesterol in mood and anxiety disorders: review of the literature and new hypotheses. *Eur. Neuropsychopharmacol.* **2004**, *14*, 135−142.
(106) Beasley, C. L.; Honer, W. G.; Bergmann, K.; Falkai, P.; Lutjohann, D.; Bayer, T. A. Reductions in cholesterol and synaptic markers in association cortex in mood disorders. *Bipolar Disord.* **2005**, *7*, 449−455.
(107) Amundson, D. M.; Zhou, M. Fluorometric method for the enzymatic determination of cholesterol. *J. Biochem. Biophys. Methods* **1999**, *38*, 43−52.
(108) Smith, P. K.; Krohn, R. I.; Hermanson, G. T.; Mallia, A. K.; Gartner, F. H.; Provenzano, M. D.; Fujimoto, E. K.; Goeke, N. M.; Olson, B. J.; Klenk, D. C. Measurement of protein using bicinchoninic acid. *Anal. Biochem.* **1985**, *150*, 76−85.
(109) McClare, C. W. F. An accurate and convenient organic phosphorus assay. *Anal. Biochem.* **1971**, *39*, 527−530.
(110) Ganguly, S.; Saxena, R.; Chattopadhyay, A. Reorganization of the actin cytoskeleton upon G-protein coupled receptor signaling. *Biochim. Biophys. Acta* **2011**, *1808*, 1921−1929.
(111) Bruns, R. F.; Lawson-Wendling, K.; Pugsley, T. A. A rapid filtration assay for soluble receptors using polyethylenimine-treated filters. *Anal. Biochem.* **1983**, *132*, 74−81.
(112) Bligh, E. G.; Dyer, W. J. A rapid method of total lipid extraction and purification. *Can. J. Biochem.* **1959**, *39*, 911−917.
(113) Aloisi, J.; Fried, B.; Sherma, J. Comparison of mobile phases for separation of phospholipids by one-dimensional TLC on preadsorbent high performance silica gel plates. *J. Liq. Chromatogr.* **1991**, *14*, 3269−3275.
(114) Baron, C. B.; Coburn, R. F. Comparison of two copper reagents for detection of saturated and unsaturated neutral lipids by charring densitometry. *J. Liq. Chromatogr.* **1984**, *7*, 2793−2801.

https://doi.org/10.1021/acschemneuro.3c00472
ACS Chem. Neurosci. 2023, 14, 3855−3868